

Supplementary Materials for

Loss of HDAC3 results in nonreceptive endometrium and female infertility

Tae Hoon Kim, Jung-Yoon Yoo, Kyung-Chul Choi, Jung-Ho Shin, Richard E. Leach, Asgerally T. Fazleabas, Steven L. Young, Bruce A. Lessey, Ho-Geun Yoon*, Jae-Wook Jeong*

*Corresponding author. Email: yhgeun@yuhs.ac (H.-G.Y.); jaewook.jeong@hc.msu.edu (J.-W.J.)

Published 9 January 2019, *Sci. Transl. Med.* **11**, eaaf7533 (2019)

DOI: 10.1126/scitranslmed.aaf7533

The PDF file includes:

Fig. S1. The expression of HDAC3 in mouse uteri during early pregnancy and in all phases of the estrous cycle.

Fig. S2. Normal ovarian histology and serum progesterone and estrogen in *Hdac3^{d/d}* mice.

Fig. S3. Decidualization defect in *Hdac3^{d/d}* mice after artificially induced decidualization.

Fig. S4. Increased collagen in the uteri of *Hdac3^{d/d}* mice.

Fig. S5. Motif analysis on HDAC3 interval sequences.

Fig. S6. Identification of *Hdac3* target genes in the mouse uterus.

Fig. S7. Recruitment of HDAC3 on *COL1A1* and *COL1A2* genes.

Fig. S8. Overexpression of collagen in the uteri of *Hdac3^{d/d}* mice.

Fig. S9. Immunohistochemical analysis of COL1 in the uteri of *Hdac3^{d/d}* mice.

Table S1. Infertility in *Hdac3^{d/d}* female mice.

Table S2. Normal ovulation and fertilization in *Hdac3^{d/d}* female mice.

Table S3. Dysregulation of atherosclerosis and fibrosis pathways in the uteri of *Hdac3^{d/d}* mice.

Table S4. List of primers used in RT-qPCR analysis.

Other Supplementary Material for this manuscript includes the following:

(available at www.sciencetranslationalmedicine.org/cgi/content/full/11/474/eaaf7533/DC1)

Table S5. Raw data (provided as an Excel file).

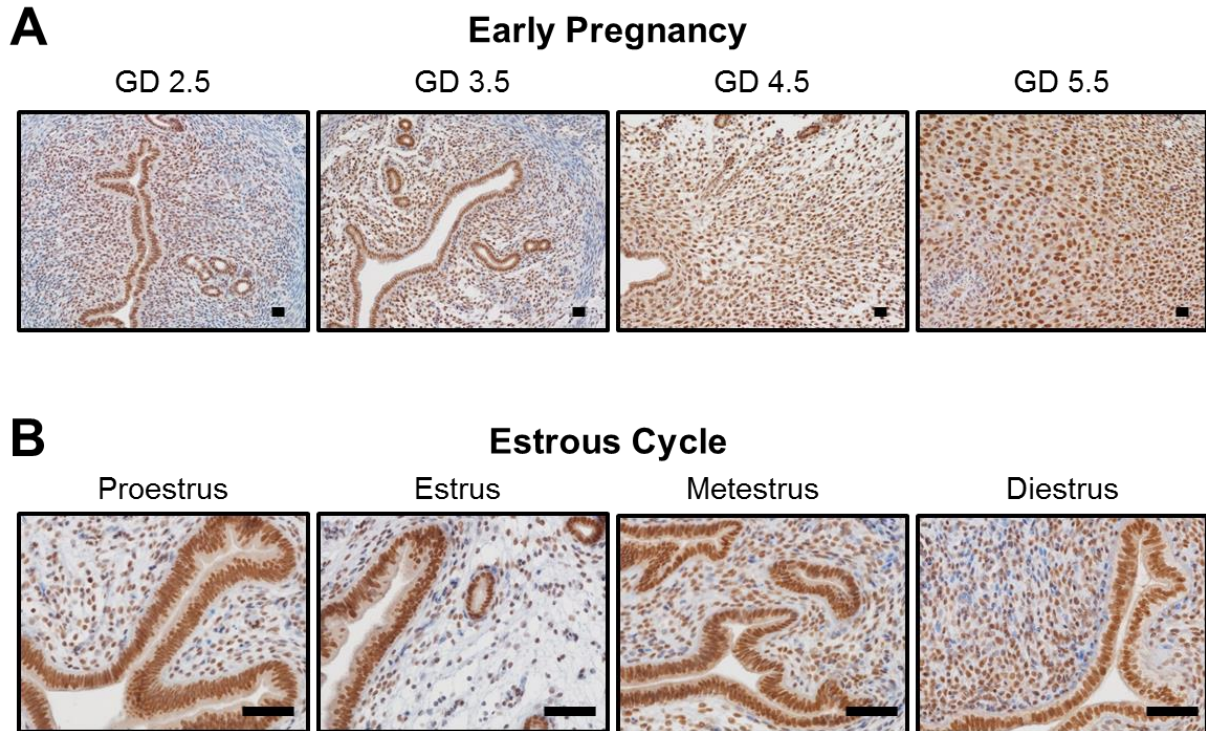


Fig. S1. The expression of HDAC3 in mouse uteri during early pregnancy and in all phases of the estrous cycle. (A) Immunohistochemical staining of HDAC3 in mouse uteri at GD 2.5, GD 3.5, GD 4.5, and GD 5.5. (B) Representative images of the immunohistochemical staining of HDAC3 in mouse uteri at different points in the estrous cycle: proestrus, estrus, metestrus, and diestrus. Nuclei were counterstained with hematoxylin. Scale bars: 50 μ m. GD, day of gestation.

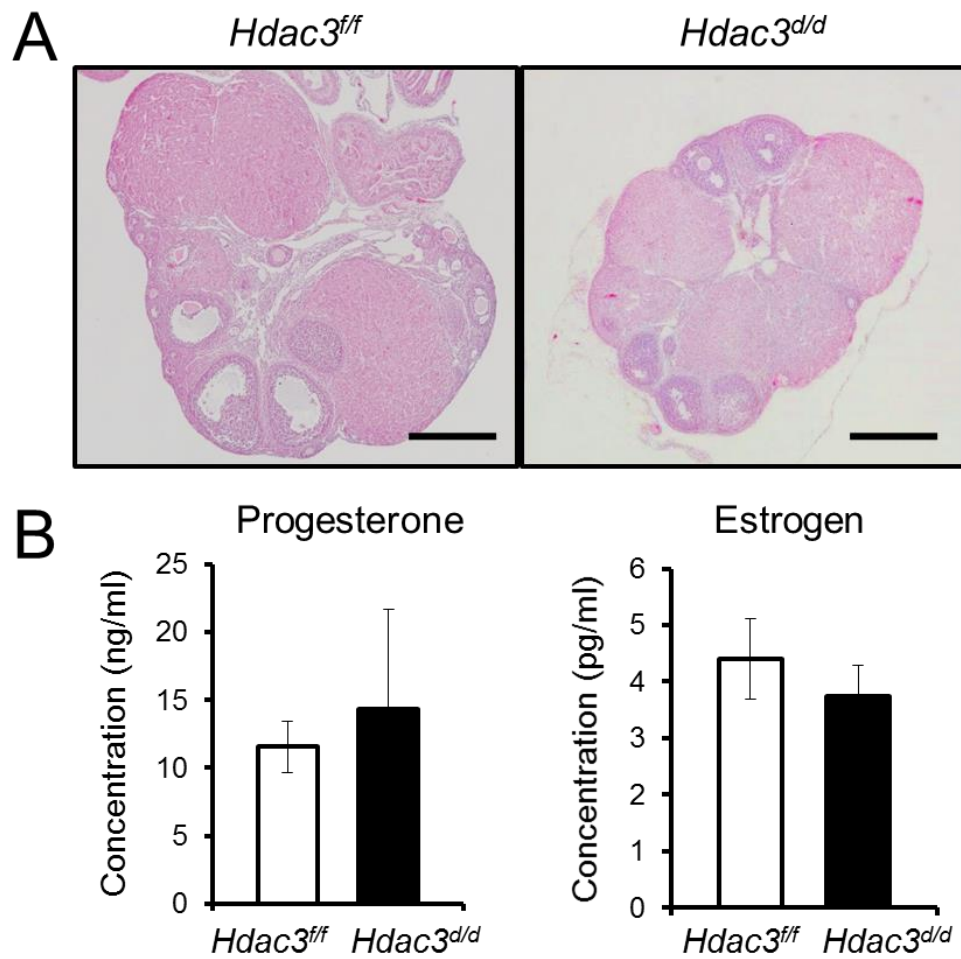


Fig. S2. Normal ovarian histology and serum progesterone and estrogen in *Hdac3^{d/d}* mice. (A) Ovarian histology by H&E staining exhibited no difference in control (*Hdac3^{ff/ff}*) and *Hdac3^{d/d}* mice. Scale bars: 500 μ m. (B) The concentrations of progesterone and estrogen were not different in the sera from control (*Hdac3^{ff/ff}*) and *Hdac3^{d/d}* mice at GD 3.5. (n = 3 for each genotype).

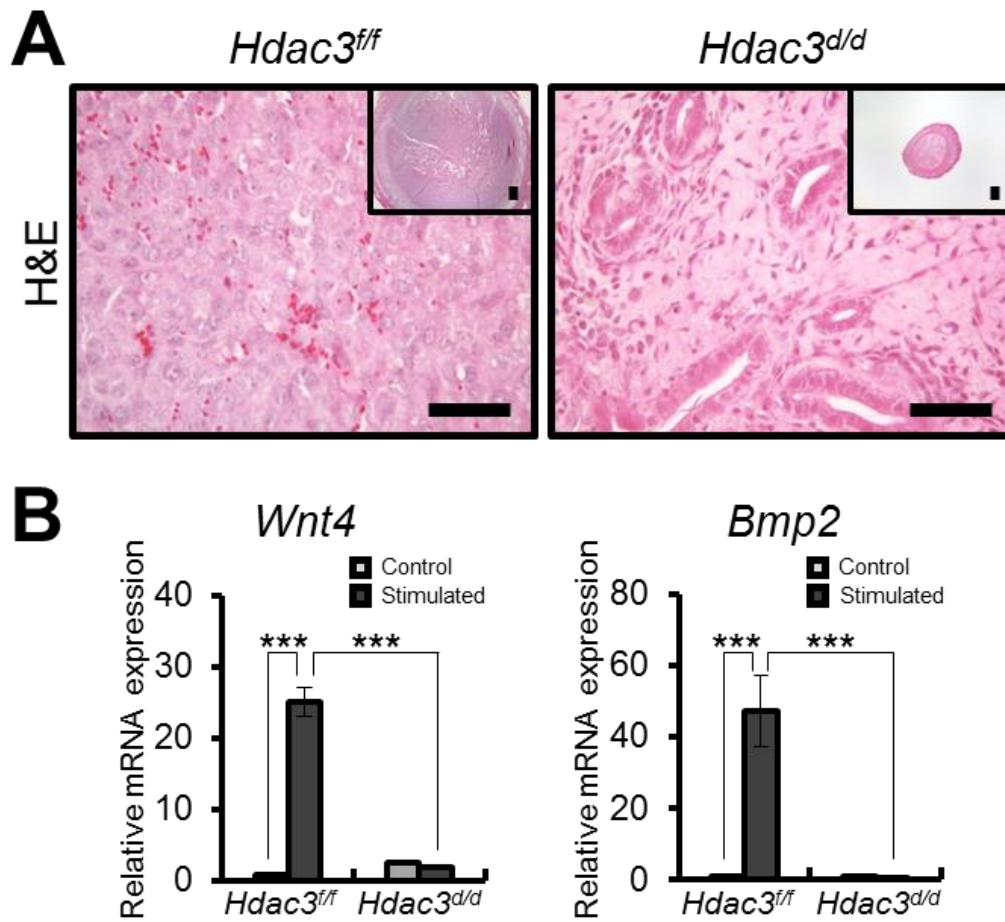


Fig. S3. Decidualization defect in *Hdac3^{d/d}* mice after artificially induced decidualization.

(A) H&E staining of uteri from *Hdac3^{ff}* and *Hdac3^{d/d}* mice after artificially induced decidualization. Scale bars: 50 µm. (B) RT-qPCR analysis of decidualization marker genes, *Wnt4* and *Bmp2*, in the uteri of *Hdac3^{ff}* and *Hdac3^{d/d}* mice after artificially induced decidualization (n = 6 for each genotype). Mean ± SEM. *** $p < 0.001$ (ANOVA followed by Tukey or Bonferroni test for pairwise t-test for data containing more than two groups.)

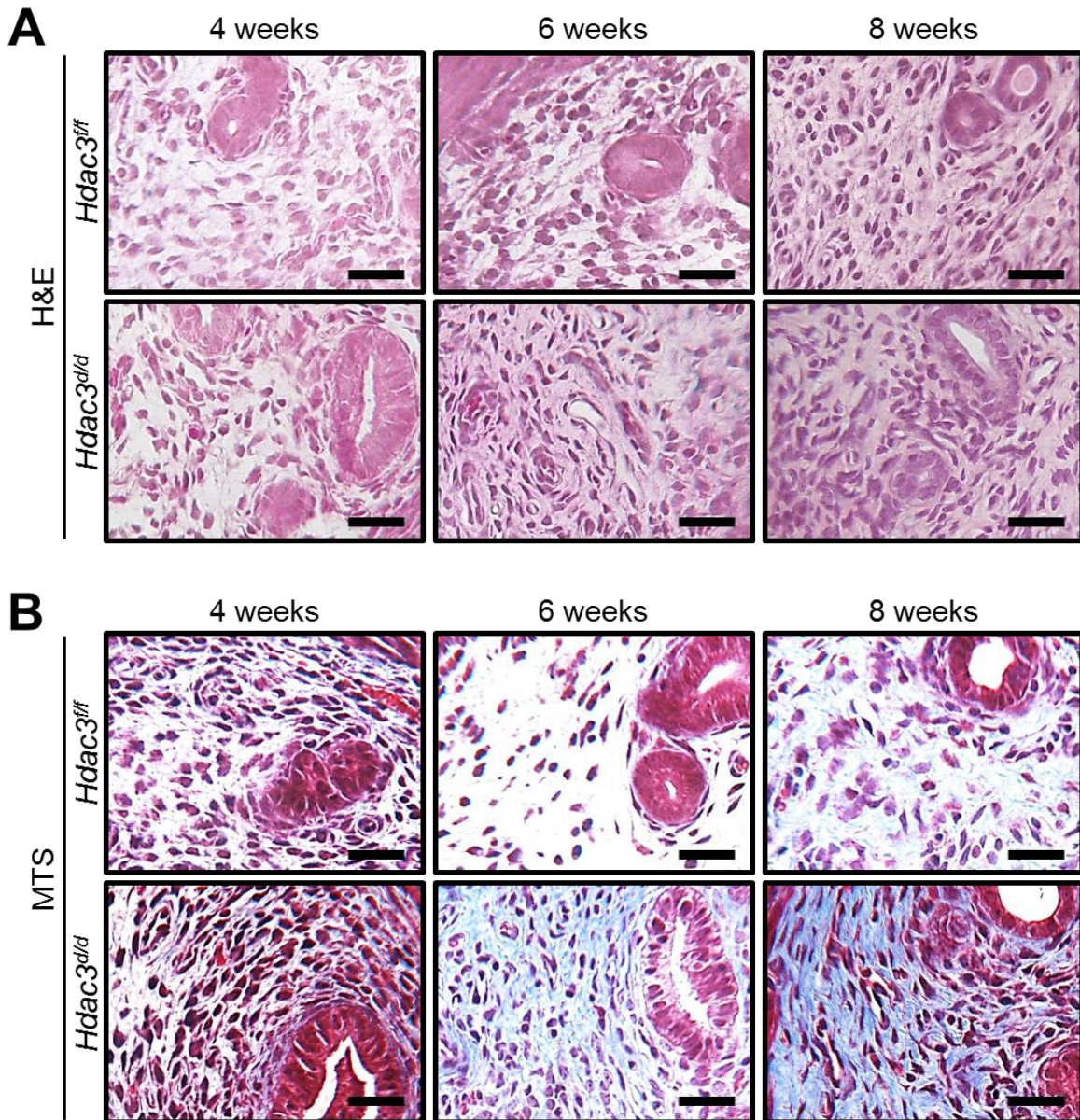


Fig. S4. Increased collagen in the uteri of *Hdac3*^{d/d} mice. (A) Hematoxylin and eosin staining of uteri from *Hdac3*^{ff} and *Hdac3*^{d/d} mice at 4, 6, and 8 weeks of age. (B) Masson's trichrome staining (MTS) of uteri from *Hdac3*^{ff} and *Hdac3*^{d/d} mice at 4, 6, and 8 weeks of age. Scale bars: 25 μ m.

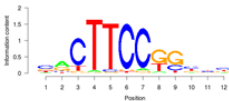
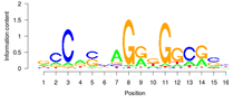
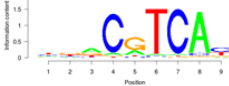
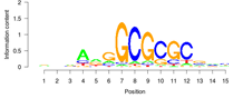
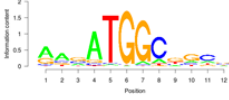
Cluster	DNA-Binding Domain Family	Motif Example	Factors
1	Ets Domain Family		GABPA, ELK1, ERG, ETV3, ELF1, ETV1, ELK3, GABPB1, Etv6, Fli1, Gm5454, ETV4, ELK4, ELF2, Etv5, EHF, Elf4, FEV, ETV7, Ets1
	Hormone-nuclear Receptor Family		RARG
	BetaBetaAlpha-zinc finger Family (zf-C2H2)		Ikzf3
2	BetaBetaAlpha-zinc finger Family (zf-C2H2)		Ctcf, CTCFL, CTCF
	BetaBetaAlpha-zinc finger Family		SP4
3	Leucine zipper Family (bZIP)		Creb1, ATF4, ATF2, ATF6, ATF1, ATF2::JUN
	Helix-Loop-Helix Family (bHLH)		E4F1
4	E2F Domain Family		E2F2, E2F3
	BetaBetaAlpha-zinc finger Family		Zfp161
5	BetaBetaAlpha-zinc finger Family (zf-C2H2)		YY1
	BetaBetaAlpha-zinc finger Family		ZFP42

Fig. S5. Motif analysis on HDAC3 interval sequences. Enriched sequence motifs identified using the Cistrome for the dataset containing HDAC3 binding in the uterus.

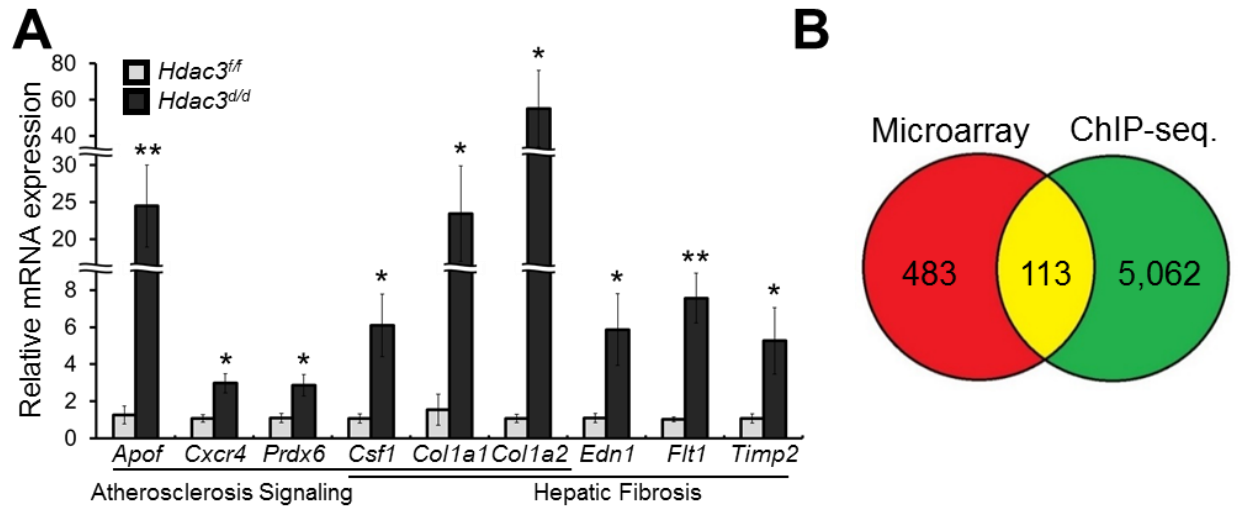


Fig. S6. Identification of *Hdac3* target genes in the mouse uterus. (A) RT-qPCR analysis of genes related to the atherosclerosis and hepatic fibrosis pathways in the uteri of *Hdac3^{fl/fl}* and *Hdac3^{d/d}* mice (n = 4 for each genotype). Mean \pm SEM. * p<0.05 and ** p<0.01, Student's t-test for data with only two groups. (B) Venn diagram illustrates the direct *Hdac3* target genes common to the ChIP-seq and microarray analyses.

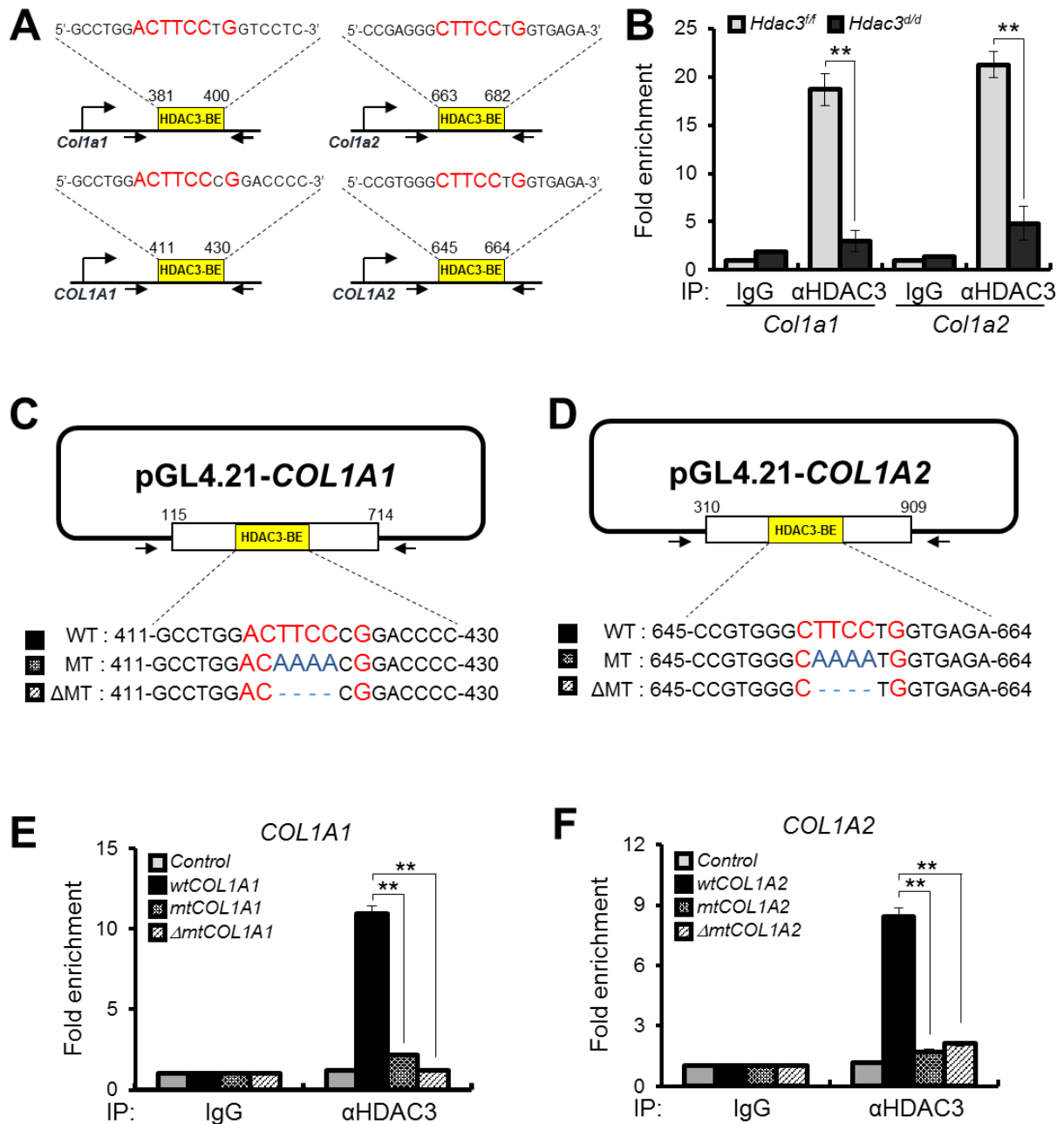


Fig. S7. Recruitment of HDAC3 on *COL1A1* and *COL1A2* genes. (A) Alignment of the HDAC3-binding element sequences of *COL1A1* and *COL1A2* genes in mouse and human. (B) The ChIP assay with uterine chromatin isolated from *Hdac3^{fl/fl}* and *Hdac3^{d/d}* mice at 6 weeks of age using IgG and HDAC3 antibody followed by RT-qPCR measurement of *Colla1* and *Colla2* (n = 3 for each genotype). (C and D) Schematic of pGL4.21-Basic plasmid including

substitutions and deletion mutations of the HDAC3-binding element on *COL1A1* (C) or *COL1A2* (D) gene. WT; wild type HDAC3-BE, MT; mutant HDAC3-BE, and Δ MT; deleted mutant HDAC3-BE. Red color indicates the conserved sequences, blue color indicates the mutated sequences, and yellow boxes indicate the locations of HDAC3 binding sites. (E and F) ChIP assay with hESCs transfected with pGL4.21-Basic (Control) and various pGL4.21-COL1A1 or pGL4.21-COL1A2 vectors using IgG and HDAC3 antibody followed by RT-qPCR measurement of *COL1A1* and *COL1A2* (n = 3 for each group). *wtCOL1A1*: pGL4.21-wild type HDAC3-BE of COL1A1, *wtCOL1A2*: pGL4.21-wild type HDAC3-BE of COL1A2, *mtCOL1A1*: pGL4.21-mutant HDAC3-BE of COL1A1, *mtCOL1A2*: pGL4.21-mutant HDAC3-BE of COL1A2, Δ *mtCOL1A1*: pGL4.21-deleted mutant HDAC3-BE of COL1A1, and Δ *mtCOL1A2*: pGL4.21-deleted mutant HDAC3-BE of COL1A2. Mean \pm SEM. ** p<0.01, ANOVA followed by Tukey or Bonferroni test for pairwise *t*-test for data containing more than two groups.

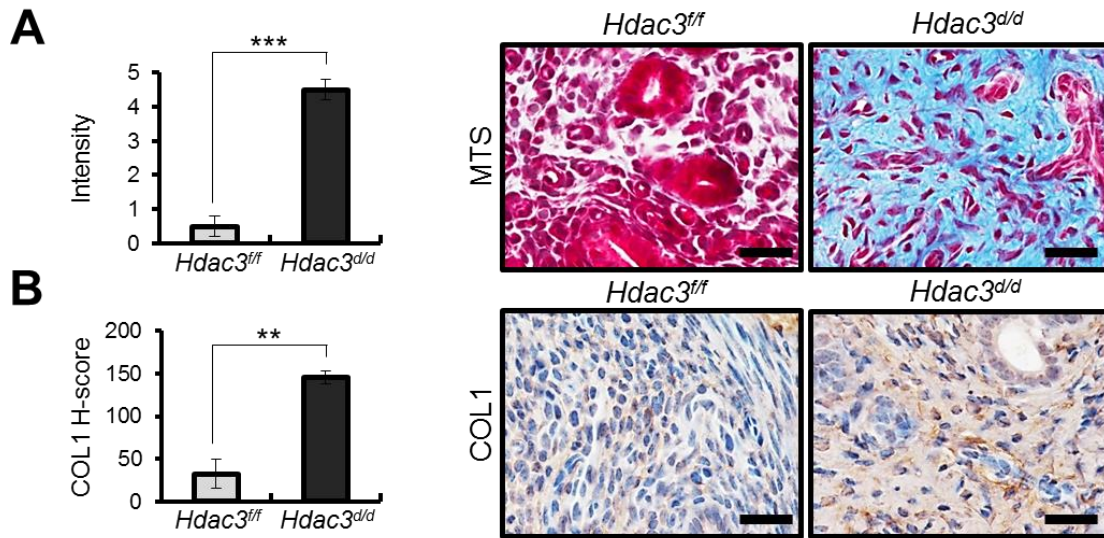


Fig. S8. Overexpression of collagen in the uteri of *Hdac3^{d/d}* mice. (A) The intensity of Masson's trichrome staining (MTS) and representative photomicrographs of *Hdac3^{ff}* and *Hdac3^{d/d}* mice at GD 3.5 (n = 3). (B) The immunohistochemical H-score and representative photomicrographs of COL1 in the uteri of *Hdac3^{ff}* and *Hdac3^{d/d}* mice at GD 3.5 (n = 3). Nuclei were counterstained with hematoxylin. Scale bars: 25 μ m. Mean \pm SEM. ** p<0.01, and *** p<0.001, Student's *t*-test for data with only two groups.

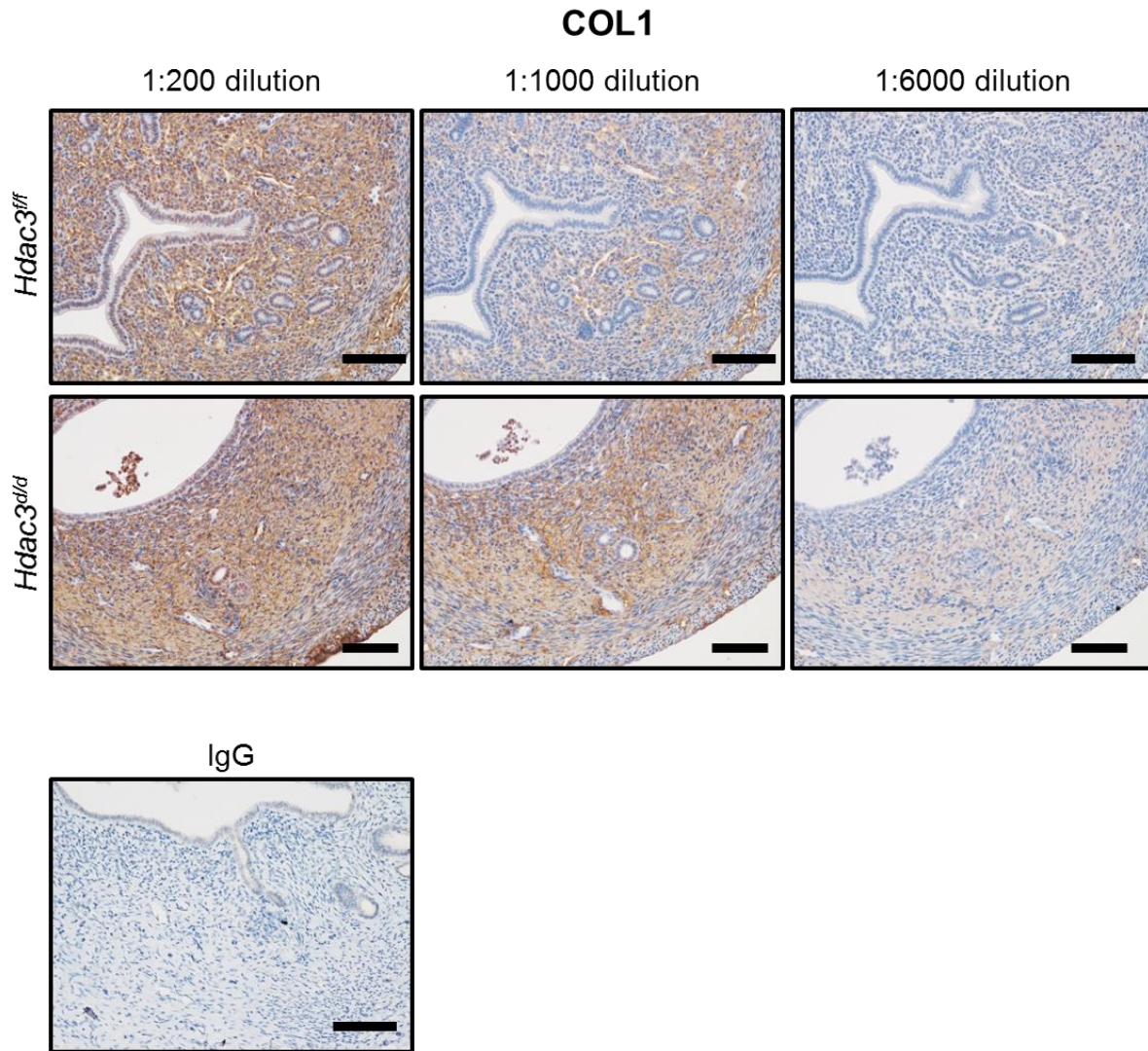


Fig. S9. Immunohistochemical analysis of COL1 in the uteri of *Hdac3^{d/d}* mice. The immunohistochemical staining of COL1 in the endometrium of *Hdac3^{f/f}* and *Hdac3^{d/d}* mice at GD 3.5 using COL1 antibody at various dilutions. The IgG antibody was used as a negative control in the mouse endometrium. Nuclei were counterstained with hematoxylin. Scale bars: 100 μ m.

Table S1. Infertility in $Hdac3^{d/d}$ female mice.

	Number of Litters	Number of Pups	Average of Pups/Litter	Average Number of Litters/mouse
$Hdac3^{ff}$ (n=5)	25	186	7.44 ± 1.09	5.00 ± 0.32
$Hdac3^{d/d}$ (n=6)	0	0	0	0

Table S2. Normal ovulation and fertilization in $Hdac3^{d/d}$ female mice.

Genotype	Total Eggs	Average Eggs / Female
$Hdac3^{ff}$ (n=7)	119	17.00 ± 4.40
$Hdac3^{d/d}$ (n=9)	170	18.89 ± 3.23

Genotype	Fertilized Eggs / Total Eggs	Fertilization Rate
$Hdac3^{ff}$ (n=3)	51 / 81	62.99%
$Hdac3^{d/d}$ (n=3)	46 / 67	68.66 %

Table S3. Dysregulation of atherosclerosis and fibrosis pathways in the uteri of *Hdac3^{d/d}* mice.

Ingenuity Canonical Pathways	Gene Name	Symbol	Accession	Fold Change
Atherosclerosis Signaling p value: 1.66E-04 Ratio: 9.4E-02	Apolipoprotein F	<i>ApoF</i>	1418239_at	1.66
	Collagen, type I, alpha 1	<i>Coll1a1</i>	1423669_at	2.12
	Collagen, type I, alpha 2	<i>Coll1a2</i>	1446326_at	2.36
	Colony stimulating factor 1 (macrophage)	<i>Csf1</i>	1460220_a_at	1.87
	Chemokine (C-X-C motif) receptor 4	<i>Cxcr4</i>	1448710_at	1.70
	Peroxiredoxin 6	<i>Prdx6</i>	1423223_a_at	1.84
Hepatic Fibrosis p value: 1.12E-02 Ratio: 6.57E-02	Collagen, type I, alpha 1	<i>Coll1a1</i>	1423669_at	2.12
	Collagen, type I, alpha 2	<i>Coll1a2</i>	1446326_at	2.36
	Colony stimulating factor 1 (macrophage)	<i>Csf1</i>	1460220_a_at	1.87
	Endothelin 1	<i>Edn1</i>	1451924_a_at	1.76
	Fms-related tyrosine kinase 1	<i>Flt1</i>	1451756_at	1.68
	TIMP metalloproteinase inhibitor 2	<i>Timp2</i>	1450040_at	1.84

Table S4. List of primers used in RT-qPCR analysis.

Gene		Primer Sequences
<i>mHdac3</i>	Forward	5'-CCGCATCGAGAATCAGAACTC-3'
	Reverse	5'-CCTTGTCGTTGTCATGGTCGCC-3'
<i>mColla1</i>	Forward	5'-GACGCCATCAAGGTCTACTG-3'
	Reverse	5'-ACGGGAATCCATCGGTCA-3'
<i>mColla2</i>	Forward	5'-GGAGGGAACGGTCCACGAT-3'
	Reverse	5'-GAGTCCGCGTATCCACAA-3'
<i>hCOLIA1</i>	Forward	5'-GGCCCAGAAGAAGTGGTACA-3'
	Reverse	5'-ATGTAGGCCACGCTGTTCTT-3'
<i>hCOLIA2</i>	Forward	5'-GATTGAGACCCTTCTTACTCCTGAA-3'
	Reverse	5'-GGGTGGCTGAGTCTCAAGTCA-3'
<i>hIGFBP1</i>	Forward	5'-CTATGATGGCTCGAAGGCTC-3'
	Reverse	5'-TTCTTGTTGCAGTTTGGCAG-3'
<i>hPRL</i>	Forward	5'-CATCAACAGCTGCCACACTT-3'
	Reverse	5'-CGTTTGGTTTGCTCCTCAAT-3'
<i>mBmp2</i>	Forward	5'-AGATCTGTACCGCAGGCACT-3'
	Reverse	5'-CGTCACTGGGACAGAACTT-3'
<i>mWnt4</i>	Forward	5'-ACAACACACACCAGTACGCC-3'
	Reverse	5'-GTTACACTTGACGTAGCAGCACCA-3'
<i>mApof</i>	Forward	5'-AGGAATGCTCTGGAGGCAGC-3'
	Reverse	5'-AACGTTTGGCCCTCTTTGGA-3'
<i>mCsf1</i>	Forward	5'-TCATGAGCAGGAGTATTGCCAA-3'
	Reverse	5'-GGCAATCTGGCATGAAGTCTC-3'
<i>mCxcr4</i>	Forward	5'-AGCCTGTGGATGGTGGTGTTC-3'
	Reverse	5'-CCTTGCTTGATGACTCCCAAAG-3'
<i>mPrdx6</i>	Forward	5'-TTGATGATAAGGGCAGGGAC-3'
	Reverse	5'-CTACCATCACGCTCTCTCCC-3'
<i>mEdn1</i>	Forward	5'-TGCTGTTCGTGACTTTCC-3'
	Reverse	5'-TGTTGACCCAGATGATGTC-3'
<i>mFlt1</i>	Forward	5'-GAGGAGGATGAGGGTGTCTATAGGT-3'
	Reverse	5'-GTGATCAGCTCCAGGTTTGAATT-3'
<i>mTimp2</i>	Forward	5'-TTCCGGGAATGACATCTATGG-3'
	Reverse	5'-GGGCCGTGTAGATAAACTCGAT-3'
<i>m18s</i>	Forward	5'-GTAACCCGTTGAACCCATT-3'
	Reverse	5'-CCATCCAATCGGTAGTAGCG-3'
<i>mLrp2</i>		Mm01328172; Applied Biosystems
<i>mFst</i>		Mm00514982; Applied Biosystems
<i>mAreg</i>		Mm00437583; Applied Biosystems
<i>mI13ra2</i>		Mm00515166; Applied Biosystems
<i>m18s</i>		4319413E; Applied Biosystems